Condensed Phase Dispersive Interactions of Benzo[*a*]pyrene with Various Solvents and with DNA: A Twist on Solvatochromism

Stephanie C. Beck and David T. Cramb*

Department of Chemistry, University of Calgary, 2500 University Drive NW, Calgary, AB T2N 1N4, Canada

Received: July 30, 1999; In Final Form: January 11, 2000

Benzo[*a*]pyrene (B(*a*)P) is a carcinogen known to interact with DNA. In this paper we explore the possibility of using spectroscopic indicators of the interaction of B(*a*)P directly with dsDNA. In so doing we have examined the solvatochromism of B(*a*)P and modeled solvent shifts based on a purely dispersive interaction. Using this model it was possible to estimate the excited-state static polarizabilities of B(*a*)P as 4.9 ($\pm$0.1) $\times$ 10^{-29}, 4.2 ($\pm$0.1) $\times$ 10^{-29}, and 5.8 ($\pm$0.1) $\times$ 10^{-29} m^3 for the S_1, S_2, and S_3 states, respectively. Moreover, we have used these polarizabilities to interpret the spectra of B(*a*)P in the presence of a 14 base-pair dsDNA oligomer in buffer solution. We provide spectral evidence that B(*a*)P and DNA interact, perhaps via intercalation.

1. Introduction

Benzo[*a*]pyrene (B(*a*)P) is a potent and prevalent environmental carcinogen found where there is incomplete combustion of hydrocarbons. For example, it is present in cigarette smoke, coal tar, and automobile exhaust. Like most polyaromatic hydrocarbons (PAHs), B(*a*)P is very hydrophobic and will partition preferentially into nonaqueous environments such as cell membranes. However, it is also known that some PAHs such as B(*a*)P can relocate between subcellular environments. The aromatic hydrocarbon receptor protein (AHR) is thought to be responsible for the transportation of PAHs to the nucleus.[1] When a PAH such as B(*a*)P traverses the cell membrane, it binds to the receptor site on AHR, held in a binding conformation by Heat-Shock Protein 90, which detaches upon ligand binding. The ligand-bound AHR associates with the aromatic hydrocarbon receptor nuclear translocator (ARNT), perhaps in the cytoplasm, to give the heterodimeric aromatic hydrocarbon receptor complex (AHRC). The complex then translocates to the nucleus, where association of some portion of the AHRC with DNA is believed to mediate carcinogenesis. B(*a*)P is thought to be a genotoxic carcinogen—it modifies the structure of DNA through the formation of an adduct. This may lead to either an altered function of the gene product or a disturbance in the regulation of expression of that product. Metabolites of B(*a*)P, notably benzo[*a*]pyrene-7,8-dihydrodiol 9,10-epoxide (BPDE), are known to alkylate nucleic acids and induce carcinogenesis in this manner. The very high biological activity of these metabolites may in part be attributed to their greater solubility in aqueous media, as well as to their "functional groups". The (+)-*anti*-BPDE isomer was studied with regard to its adduct formation with DNA, which is believed to be a multistep process.[2] The step preceding covalent reaction is generally thought to involve the physical insertion of BPDE between two base pairs of the DNA, or *intercalation*. It is therefore possible that unmodified B(*a*)P may intercalate as well, particularly considering its low solubility in aqueous media. Evidence for B(*a*)P intercalation has been sought by various means.

There are a few studies in the literature that have attempted to determine whether B(*a*)P intercalates with DNA: Ridler and Jennings[3] performed electrooptical fluorescence studies in which DNA molecules in solution were aligned parallel to an applied electric field. Transient changes in the polarized components of B(*a*)P's emitted fluorescence were measured. Results were consistent with intercalation of B(*a*)P, but were not conclusive. Green and McCarter[4] carried out similar experiments using flow orientation to align the DNA. Characteristic changes in intensity of polarized fluorescence were also observed. However, the B(*a*)P was solubilized with caffeine in these experiments. This may have affected B(*a*)P's DNA-binding properties: benzo[*a*]pyrene associates with caffeine via van der Waals forces to form a sandwich structure with caffeine on both sides.[5] There are indications, however, that the interaction between pyrene and caffeine are as weak as those with solvent molecules; B(*a*)P may therefore act as a free molecule. Results were again consistent with intercalation of B(*a*)P, but further study is required.

Although fluorescence resonance energy transfer could in principle be used to determine the nature of B(*a*)P−DNA interactions, there are some caveats, as shown in the recent literature. Hyun et al.[6] found that the minor groove binding ligands, DAPI (4′,6-diamidino-2-phenylindole) and Hoechst 33342 (2′-[4-ethoxyphenyl]-5-[4-methyl-1-piperazinyl]-2,5′-bi-1*H*-benzimidazole), gave results similar to those observed for known DNA intercalators. Caution must therefore be used when interpreting energy transfer in terms of DNA intercalation.

It is well-known that the emission spectra of many relatively nonpolar fluorophores, including C_{60}[7] and azulene,[8] are sensitive to the nature of the surrounding environment (i.e., polarity, polarizability). Moreover, this solvatochromism has been used to detect binding to macromolecules and/or to describe the polarity of the binding sites, as in the case of 1-anilino-8-naphthalenesulfonic acid (ANS) bound to apomyoglobin.[9] We propose to use the spectral characteristics of B(*a*)P in various environments to construct a spectroscopic tracing method that will allow us to assess how unmodified B(*a*)P interacts with DNA. This will eventually lead to an in vivo spectroscopic tracing protocol. As mentioned above, the metabolite BPDE appears to intercalate as the first step in adduct formation, as evidenced by initially negative linear dichroism of the BPDE chromophore. In a living cell, metabolites of B(*a*)P will almost certainly be present along with unmodified B(*a*)P. However,

10.1021/jp992707h CCC: $19.00
Published on Web 03/02/2000

the chromophore present in BPDE has essentially the same spectral properties as pyrene. Pyrene's emission spectrum is sufficiently different from that of benzo[*a*]pyrene to allow the differentiation of B(*a*)P and its metabolites.

To our knowledge, there is very little, if any, work in the recent literature that exploits the solvatochromic shifts in B(*a*)P's emission spectrum to detect its intercalation into DNA. Shifts in the emission spectrum occur due to both general and specific solvent effects. General solvent effects arise from interactions between the electrons of an excited fluorophore and the reactive fields induced in the surrounding solvent. The strength of these effects depends on the excited-state electronic configuration and on the refractive index, n (i.e., the polarizability) and the dielectric properties, ϵ, of the solvent.

In the late 1950s a number of models were introduced in order to predict solvatochromic behavior. In his seminal paper, McCrae described the extent to which the energy difference between the ground electronic state and the excited electronic state will vary with solvent.[10] It was revealed that the electric dipole moment (μ) of a molecule in the excited state can thus be determined from the spectral shifts observed in various solvents. Spectral shifts arising from specific solvent effects are often much larger than those due to general interactions. Specific solvent-fluorophore interactions include hydrogen bonding and complexation. These effects depend greatly on the chemical structures of the fluorophore and the solvent and are thus difficult to model on the basis of generalized solvent parameters such as n and ϵ.

Capomacchia et al.[11] investigated the solvatochromism of B(*a*)P and of two of its monohydroxy metabolites. The findings from this study indicate the weak physical interactions between B(*a*)P and solvent molecules are comparable in magnitude to the interactions present in the proposed intercalated B(*a*)P−DNA complex in aqueous solution. Ten different solvent scales were examined with regard to the results obtained, including Kamlet and Taft's π^* scale.[12] The results obtained suggest that the π^* parameter is weighted in favor of the polarizability factor. However, no correlation greater than 0.87 was observed even for the π^* scale. Nevertheless, it was revealed that solvation data could provide clues as to the nature of the DNA interaction process. In particular, the stabilizing effect of pyridine on B(*a*)P's emission spectrum points to the fact that three components may be involved at the intercalation site that contains a heterocyclic ring nitrogen, an aromatic π-electron system and a permanent dipole moment.

To use solvatochromic arguments to decipher DNA−B(*a*)P interactions, a solvent−solute coupling model physically relevant to nonpolar B(*a*)P needs to be developed. From this one can understand how the features of B(*a*)P's excitation and emission spectra provide information on the nature of its environment.

In this paper, we present the results of a study of the solvatochromism of B(*a*)P fluorescence in a variety of solvents. The results have been modeled using the dipole and dispersion interactions. On the basis of these results, we propose a model involving the change in static polarizability to account for B(*a*)P's solvatochromic shifts and to determine the polarizability of the S_1, S_2, and S_3 states of B(*a*)P. We then use the S_1 polarizability to assess the nature of the binding site for B(*a*)P on a 14 base pair double-stranded DNA oligonucleotide.

2. Experimental Methods

All fluorescence spectra were collected using a Photon Technology International (Canada) LPS-220 spectrofluorometer fitted with a xenon arc lamp. All optical cuvettes were Suprasil quartz (Hellma). Unless otherwise noted, the following chemicals were used without further purification: Benzo[*a*]pyrene was obtained from Professor A. Okey at the University of Toronto. Dibasic anhydrous sodium phosphate (Na_2HPO_4) was purchased from J. T. Baker Chemical Co. Monobasic sodium phosphate monohydrate ($NaH_2PO_4 \cdot H_2O$) was purchased from Fisher Scientific Co. Sodium chloride and disodium EDTA were purchased from BDH, Inc. as well. Tris was purchased from ICN Biomedicals, Inc., and converted to Tris·HCl prior to use. Desalted oligonucleotide 14-base pair DNA (sequence: ATATAAATTTATAT) was purchased from the University of Calgary DNA services and was dissolved in TE buffer and annealed prior to use. All water used was ultrapure (Barnstead Nanopure 3000). The following solvents were used as purchased: methanol (OmniSolv, EM Science); ethanol (absolute); cyclohexane (OmniSolv, BDH, Inc.); *n*-heptane (OmniSolv, EM Science); toluene (OmniSolv, BDH, Inc.); dimethyl sulfoxide (DMSO, Anal-R; BDH, Inc.), tetrahydrofuran (THF, OmniSolv, EM Science), acetonitrile, acetone, ethylene glycol, dimethylformamide, diethyl ether, *n*-heptane, and chlorobenzene (OmniSolv, BDH, Inc.).

Phosphate Buffer. Dibasic sodium phosphate was dried in an oven at 120 °C for several hours prior to use. $NaH_2PO_4 \cdot H_2O$ (4.160 g, 30.2 mmol) and Na_2HPO_4 (2.821 g, 19.9 mmol) were added to a 500 mL volumetric flask and diluted with ultrapure water. Final pH 6.7 ± 0.1.

Tris/EDTA (TE) Buffer. A 1 M pH 7.61 Tris·HCl solution was prepared as follows: Tris (24.243 g, 0.2 mol) was diluted to 200 mL with 2 M HCl(aq) (69.4 mL) and the balance ultrapure water. A 0.5 M pH 7.60 EDTA solution was prepared by dissolving EDTA (37.220 g, 0.1 mol) in 200 mL of ultrapure water with 16 M NaOH to pH 7.60, with stirring and gentle heating. TE buffer was prepared by mixing Tris·HCl solution (2 mL) and EDTA solution (0.4 mL) with ultrapure water and diluting to 200 mL for a final pH of 7.60.

Solutions of B(*a*)P. Aliquots (10 μL) of a 1 mM B(*a*)P/toluene stock solution were placed in scintillation vials, and the solvent was removed with a stream of dry nitrogen. The solvents (10 mL) were pipeted into the vials and the solutions stirred overnight in the dark.

11 μM 14-Base Pair DNA in pH 7.6 TE Buffer. A sample of single-stranded 14-base pair DNA (ssDNA) (1980 μg, 2.17×10^{-7}mol) was added to a 10 mL volumetric flask and diluted to volume with TE buffer. The solution was heated, with stirring, from 30 to 70 °C (5 min at 70 °C) to anneal. The solution was then allowed to cool slowly to room temperature with stirring. Final concentration dsDNA: 10.9 μM.

1 μM B[*a*]P/1 μM 14-Base Pair DNA in pH 7.6 TE Buffer. A stock solution of B(*a*)P in toluene (1 mM) was prepared. An aliquot (10 μL) was micropipeted into a scintillation vial and the solvent removed with a stream of dry nitrogen. Then 10 mL of 14bp DNA (10.9 μM) was added and the solution stirred in the dark for several days.

3. Results and Discussion

Solvatochromism. The effect of solvent−solute interactions on the solute spectral properties (i.e., solvatochromism) has been previously described using two fundamentally different approaches. In the first, the system is modeled quantum mechanically using second-order perturbation theory applied to the solute transition energies.[13,14] This approach considers both electric dipole induced interactions and dynamic dispersive interactions induced by the transition moment of the solute. In the second,

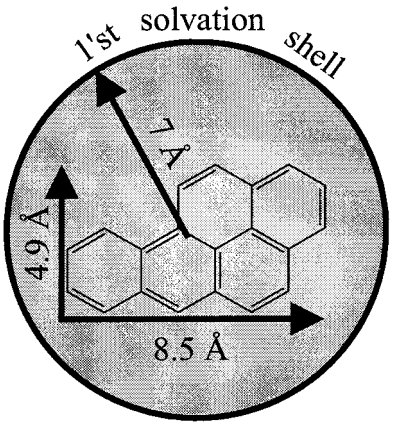

Figure 1. Carbon backbone of benzo[*a*]pyrene inside a cavity of radius 7 Å. The radius is estimated on the basis of the structure of B(*a*)P.

solvation energy terms are introduced phenomenologically to the ground and excited electronic states.[15] In this approach, the electric dipole interactions are considered to be dominant. In the Lippert−Mataga approach[16] the dependence of the Stokes shift on solvent is used to determine the excited-state electric dipole moment.

We observed no discernible solvent dependence in the Stokes shift. This could mean that either there is no electric dipole moment developed in the excited state of B(*a*)P or that interactions occur as the solvent reorients, which offset the interactions relevant to the absorption process. We have, however, observed solvent dependent shifting of both the absorption features and the fluorescence spectra separately (see below). This suggests that there are indeed solvent sensitive changes in the excited-state electronic properties of B(*a*)P. To determine the nature of this solvatochromism, we have attempted to model them considering changes in either B(*a*)P electric dipole moment or polarizability.

For both models, the size of the cavity that B(*a*)P occupies in solution must be estimated. We have used the structure of B(*a*)P to estimate the cavity size. From the X-ray structure,[17] it can be shown that the longest axis of B(*a*)P is approximately 12 Å. We have simply added 1 Å to both ends of this axis to give a cavity radius of 14/2 or 7 Å. The cavity is depicted in Figure 1.

In Figure 2, the fluorescence and excitation spectra are given for B(*a*)P in *n*-hexane. It is worthwhile noting some of the features of these spectra. First, the excitation and emission spectra display reasonable, but not perfect, mirror symmetry. This is suggestive that the ground- and excited-state nuclear geometries are different, but not significantly. The excited states of B(*a*)P have been assigned[18] according to their transition dipole polarizations in analogy with pyrene. Also, the features of the emission spectrum are believed to be vibrations or combinations of vibrations possessing favorable Franck−Condon overlap with those of the ground singlet state. The spacing of the progression is approximately 1300 cm^{-1} and with the exception of aqueous solutions, does not change significantly with solvent. This vibrational energy is similar to that for aromatic ring-breathing modes.[19]

Sample excitation and emission spectra for B(*a*)P in various solvents is presented in Figures 3a,b. The spectral positions of the transitions in question were determined by fitting a Gaussian function to the feature used. The peak positions are listed in Table 1.

The shifting of either the absorption features or the emission features can be modeled by the interactions of the solute dipole

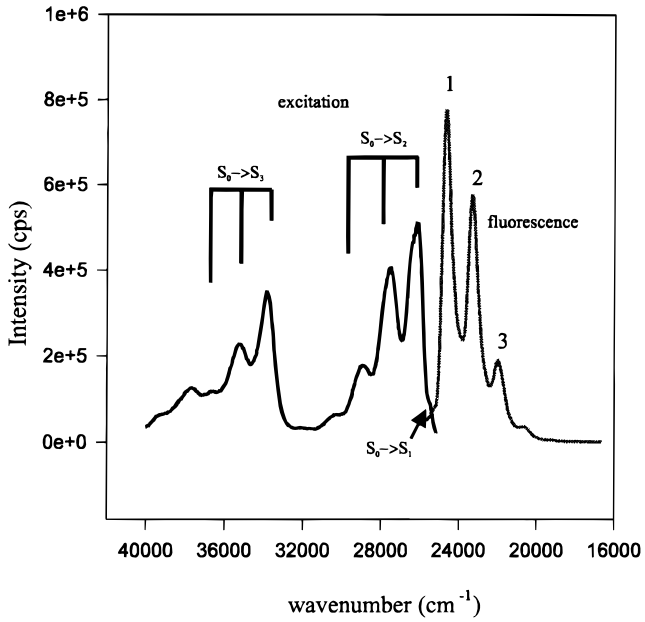

Figure 2. Overlay of the excitation (dark line) and fluorescence spectra (light line) of benzo[*a*]pyrene at 1×10^{-6} M in *n*-hexane. The excitation spectrum was collected with the emission tuned to 24 550 cm^{-1} (410 nm), whereas the fluorescence spectrum was collected at an excitation energy of 26 320 cm^{-1} (380 nm).

with the solvent and/or the dispersion interactions between the solute and solvent. Thus, the changes in energy associated with these interactions are written

$$\Delta\nu(\text{solvated}) = \Delta\nu(\text{vacuum}) + \Delta\nu(\text{dipole}) + \Delta\nu(\text{dispersion}) \quad (1)$$

We will examine the two types of interactions separately. In the first and most traditional approach, one assumes that the solvent-induced shifting of excitation and of fluorescence spectral features arise from a change in electric dipole moment for the excited state. Moreover, since there is no trend in the Stokes shift versus the solvent low-frequency dielectric characteristics, ϵ, the interaction between B(*a*)P and the solvent can be defined solely in terms of the solvent high-frequency dielectric properties (i.e., the refractive index, *n*).[10] Accordingly, in the absence of solvent reorientation the spectral shift for absorption or emission can be written[10]

$$\Delta\nu(\text{solvated}) = \Delta\nu(\text{vacuum}) + \frac{1}{hc}\frac{(\mu_{S_0}{}^2 - \mu_{S_n}{}^2)}{a^3}\left(\frac{n^2-1}{2n^2+1}\right) \quad (2)$$

where μ_{S_0} and μ_{S_n} are the ground and excited electronic state electric dipole moments, respectively, *h* is Planck's constant, *c* is the speed of light, *a* is the Onsager radius of the solute cavity, and $\Delta\nu$ is the energy of the transition.

Using the above model, we plotted the energy changes in absorption spectral maxima versus *f(n)*, where

$$f(n) = \left(\frac{n^2-1}{2n^2+1}\right)$$

These plots are presented in Figure 4a−c. It is clear that a trend exists. From the slope of these graphs, one can determine the excited-state electric dipole moments assuming a cavity radius of 7 Å. Fluorescence emission shifts relative to methanol were plotted against $(n^2 + 1)/(2n^2 - 1)$ for the peak labeled 1

TABLE 1: Data Used in the Calculations of Solvatochromic Shifts for Benzo(*a*)pyrene in Various Solvents

solvent	n^a	l^a + 0.5 (Å)	w^a + 0.5 (Å)	area (Å^2)	z	$10^{19}I_0$ (J)^a	$10^{19}I_n$ (J)^a	α_2 (m^3)^a	S_1 (cm^{-1})	S_2 (cm^{-1})	S_3 (cm^{-1})
water	1.333	2.015	1.087	2.19	281	6.31	4.40	1.47×10^{-30}	24530	26100	33880
acetonitrile	1.344	3.762	2.322	8.74	70	7.26	4.84	2.96×10^{-30}	24540	26100	33900
methanol	1.328	2.879	2.296	6.61	93	6.90	4.68	3.27×10^{-30}	24630	26250	33570
ethanol	1.361	3.876	3.179	12.32	50	6.80	4.63	5.48×10^{-30}	24600	26200	33570
ethylene glycol	1.432	5.604	2.253	12.63	49	6.71	4.59	5.70×10^{-30}	24480	25850	33580
acetone	1.359	4.397	4.286	18.85	33	6.58	4.53	6.37×10^{-30}	24540	26100	
DMF	1.431	4.320	3.876	8.91	42	6.41	4.45	7.81×10^{-30}	24480	25900	33600
diethyl ether	1.353	6.45	2.298	14.82	42	6.55	4.52	9.47×10^{-30}	24600	26170	33900
benzene	1.501	5.458	6.672	36.42	17	6.43	4.46	1.05×10^{-29}	24480	25850	33440
cyclohexane	1.427	5.728	5.028	28.80	21	6.63	4.56	1.09×10^{-29}	24640	26150	33420
n-hexane	1.375	8.03	2.643	21.22	29	6.79	4.63	1.19×10^{-29}	24650	26200	33840
toluene	1.496	7.005	6.672	46.74	13	6.76	4.62	1.23×10^{-29}	24480	25850	33120
chlorobenzene	1.524	6.124	4.794	29.36	21	6.39	4.44	1.32×10^{-29}	24440	25750	33380
n-heptane	1.388	9.286	2.643	24.54	25	6.64	4.56	1.37×10^{-29}	24680	26250	33470
THF	1.405	4.084	3.366	13.75	45	6.59	4.54		24550	26000	33680

[a] Values taken from ref 41.

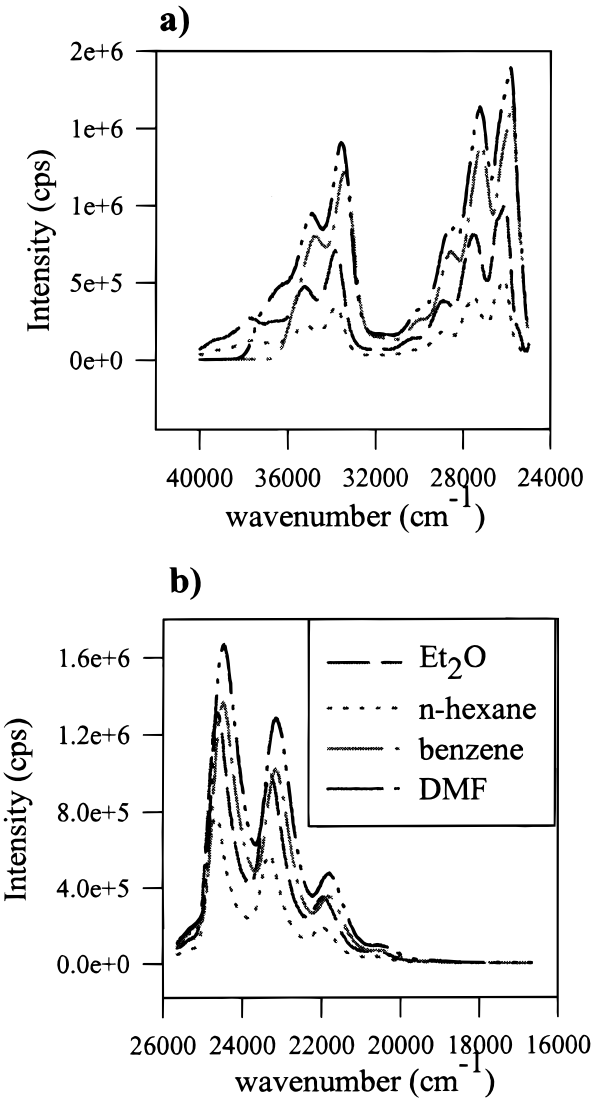

Figure 3. (a) Series of excitation spectra of benzo[*a*]pyrene in various solvents. (b) Series of fluorescence spectra of benzo[*a*]pyrene at 1×10^{-6} M in various solvents. The excitation spectrum was collected with the emission tuned to 24 550 cm^{-1} (410 nm), whereas the fluorescence spectrum was collected at an excitation energy of 26 320 cm^{-1} (380 nm).

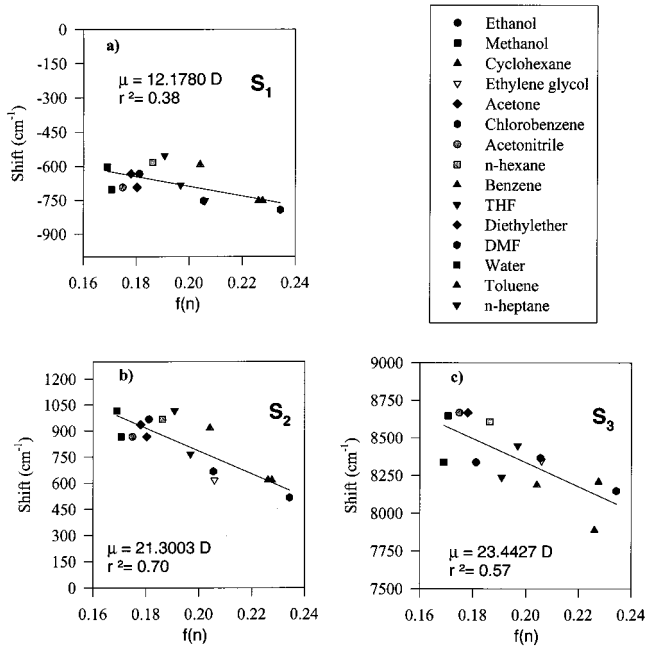

Figure 4. (a) Plot of the shift of feature 1 in the fluorescence spectrum from the 0−0 transition versus $(n^2 - 1/2n^2 + 1)$ for various solvents. (b) and (c) Plots of the shift of the 0−0 transition spectrum from the 0−0 transition versus $(n^2 - 1/2n^2 + 1)$ for various solvents for the $S_0 \rightarrow S_2$ and $S_0 \rightarrow S_3$, transitions, respectively. Using eq 1, the slopes of these plots reveal the excited-state dipole moments μ. The R^2 values for the linear regression of these plots are also displayed.

(Figure 2). Excitation shifts relative to methanol for peaks 1 and 2 (Figure 2b) were also plotted against $(n^2 + 1)/(2n^2 - 1)$. The values of μ obtained are 12, 21, and 23 D for the S_1, S_2, and S_3 states, respectively. In comparison with the values of μ obtained above, the molecule PRODAN, 6-propionyl-2-(dimethylamino)naphthalene, has an excited-state dipole moment of ca. 10 D.[20] This dipole is thought to result from charge separation "between" the amino and carbonyl groups. B(*a*)P has no such functional groups that would favor charge separation, and so it seems that the electric dipole moments thus determined are far too large to be plausible. Indeed, we have calculated the ground and first excited singlet state electric dipole moments for B(*a*)P using Gaussian 98 (STO-3G basis set)[21] and determined them to be negligible. For S_0, we calculate 0.05 D and for S_1, 0.02 D. Thus, although a trend in the excitation and fluorescence spectral features versus solvent refractive index was observed, it is not due to static dipole−solvent interactions. The fact that the refractive index is related to the solvent's molecular polarizability suggests that dispersion (or London) interactions may be the dominating effect in the observed spectral shifts.

Our static dispersion model is based on the premise that the energies of the excited electronic states shift with respect to the ground-state energies owing to changes in the London interaction.[22,23] To estimate the energy for one solvated solute molecule, we will consider only pairwise interactions including the first solvent shell. Our approach differs from that of Kettley et al.[23] in that we consider the excited-state polarizabilities for the solute as depending on both the proximity to the ionization potential and the electron configuration. For *z* equivalent solvent molecules, the energy of the solute molecule in electronic state a becomes

$$E_a(\text{solvated}) = E_a(\text{vacuum}) - z\frac{3}{2}\frac{\alpha_1^a\alpha_2}{R^6}\frac{I_1I_2}{I_1+I_2} \qquad (3)$$

where α_1 and α_2 are the isotropic polarizabilities of the solute and solvent, respectively, I_1 and I_2 are their first ionization energies, and R is the center to center distance of the two interacting bodies. The change in this term arises from a change in the solute polarizability, α_1, for the solute in an excited electronic state. We label this $\alpha_1^{S_n}$. The transition energy for excitation from the ground electronic state, S_0, to some excited electronic singlet state, S_n, is

$$\Delta\nu(\text{solvated}) = \Delta\nu(\text{vacuum}) - z\frac{3}{2}\frac{\alpha_2}{R^6}\left(\alpha_1^{S_n}\frac{I_1^{S_n}I_2}{I_1^{S_n}+I_2} - \alpha_1^{S_n}\frac{I_1I_2}{I_1+I_2}\right) \qquad (4)$$

where

$$I_1^{S_n} = I - E_{S_n}$$

The result presented in eq 4 is similar in form to that of Longuet-Higgins and Pople.[14] The difference is that they related the solvent shifts to the ground-state solute−solvent dispersion interactions and to the transition dipole moment into the excited state in question, whereas our second term represents the static dispersion interaction between the excited-state solute and ground-state solvent. In fact, the effect of transition dipole moment should be vanishing except where the external electric field is resonant with both the solute and the solvent. Equation 4 is analogous to that presented by Iweibo et al.[24] as derived by Abe,[25] with the exception of the method of determining *z* and *R*. In Abe's approach *z* and *R* are determined by assuming that the solvent and solute molecules are spheres of appropriate van der Waals radii.

For ease of data reduction and presentation, we will gather some constants together:

$$l_0 = \frac{I_1I_2}{I_1+I_2} \qquad l_n = \frac{I_1^{S_n}I_2}{I_1^{S_n}+I_2} \qquad B = \frac{3}{2}z\frac{\alpha_2}{R^6}$$

and rearrange eq 4 to yield

$$\frac{\Delta\nu(\text{solvated}) - \Delta\nu(\text{vacuum})}{Bl_n} - \alpha_1^{S_0}\alpha_2\frac{l_0}{l_n} = -\alpha_1^{S_n}\alpha_2 \qquad (5)$$

A plot of the left-hand side, which we will call the *reduced absorption shift*, versus the solvent polarizability, α_2, can be used to determine the excited-state polarizability, $\alpha_1^{S_n}$, of B(*a*)P. Such plots can be found in Figure 5a−c.

The values of the parameters used for the various solvents are presented in Table 1. To estimate the number of molecules

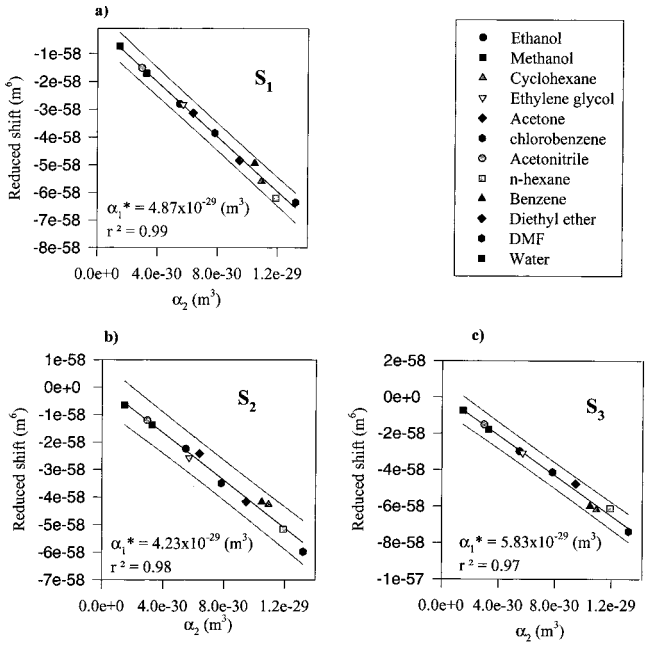

Figure 5. Plots of the reduced shift as determined by eq 7 versus solvent polarizabilities. Panels a−c represent the S_1, S_2, and S_3 excited states, respectively. Also displayed are the linear regressions (center lines) and the 99% confidence intervals (two outer lines).

in the first solvent shell, we have calculated the largest area that the solvent molecules project. This is done using the ground electronic state structures of the molecules and adding 0.5 Å to the length of each axis to account for the average intermolecular spacing of the molecules with respect to their the van der Waals radii and thermal motion. Using this area, the solvent molecules are then tiled on a sphere of radius 7 Å around B(*a*)P until no more space is available in the first solvation shell. This was used as the simplest starting point for our calculations. The polarizabilities used for the solvent molecules are considered to be isotropic. The ground electronic state polarizability for B(*a*)P was taken from the work of White and Schmidt.[26]

The shifting energies of the $S_0 \rightarrow S_2$ and $S_0 \rightarrow S_3$ transitions are calculated using the first peaks of their respective excitation spectra. The band origin for the $S_0 \rightarrow S_1$ is very weak and therefore difficult to measure accurately. Therefore, we have used peak 1 of the fluorescence spectrum. Because it has been shown that peak 1 in the fluorescence spectrum does not represent the band origin (i.e., 0−0 in the vibrational progression) for this transition,[27] we have therefore added 508 cm^{-1} (the energy difference between the band origin[25] and the first intense feature of the fluorescence spectrum) to peak 1 for our plots. The vacuum energies of the $S_0 \rightarrow S_2$ and $S_0 \rightarrow S_3$ transition origins are taken from Greenblatt et al.[28]

Consider Figure 5a. A linear regression to the data produces an excited-state polarizability of 4.9 (±0.1) × 10^{-29} m^3 for B(*a*)P in its first excited state. This is approximately 1.4 times the value of the ground-state polarizability (3.6 × 10^{-29} m^3). The correlation of the fit, including all data, is 0.99. From Figure 5b,c, the excited-state polarizabilities for S_2 and S_3 have been determined as 4.2 (±0.1) × 10^{-29} m^3 and 5.8 (±0.1) × 10^{-29} m^3, respectively. It must be noted that the highest value for the excited-state polarizability is determined using this method because we use the smallest number of molecules necessary to fill the first solvation shell. From Figure 5, it appears that the model works remarkably well for B(*a*)P. This may be because of the inherent lack of a significant electric dipole moment in any electronic state of B(*a*)P. Moreover, this model is completely

general regardless of whether the individual solvent molecules themselves possess electric dipole moments. It is possible that dipole−induced dipole interactions occur in the B(*a*)P system. However, these interactions are generally smaller than the London interactions involving B(*a*)P[29] and may in fact average to zero if there is random solvent orientation within the first solvation shell.

It has been previously observed that the solvatochromic shift for nonpolar molecules in solvents scales with the transition intensity or transition dipole.[30] We do not observe this for B(*a*)P. The S_3 state displays the largest solvatochromic shifting although it is not the most intense feature. The relative values of the polarizabilities follow the relative magnitudes of the shifts. According to the definition of static polarizability,[21] the differences in polarizabilities must represent a tradeoff between the electron density distributions and proximities to the ionization potential for each electronic state. All of the excited states possess polarizabilities greater than that of the ground state. This would certainly result from their closer proximity to the ionization threshold.

The values of the excited-state polarizabilities have been determined only for a few polyaromatic molecules. For example, Iweibo et al.[23] have used solvatochromism to examine excited-state polarizabilities of analine, phenol, and naphthalene. They determined the polarizabilities for the ^1L_a, ^1L_b, and ^1B_b states of naphthalene to be 2.7×10^{-29}, 3.6×10^{-29}, and 7.1×10^{-29} m^3, respectively, compared with a ground-state value of 1.6×10^{-29} m^3. These values are of the order predicted using cubic response theory[31] but tend to be larger than predicted. This is perhaps owing to the nature of determining the number of solvent molecules. Additionally, degenerate four-wave mixing was used to measure α^* for C_{60} in toluene.[32] The real part of the excited-state polarizability for C_{60} was determined to be 1.2×10^{-28} m^3 compared with 7×10^{-29} m^3 in the ground electronic state. This is a reasonable comparison to that of B(*a*)P, since for ground electronic states the polarizabilities scale with molecular volume. A more traditional technique used to measure excited-state polarizabilities is condensed-phase laser Stark spectroscopy.[33] Recently, the elegant technique of higher-order Stark spectroscopy has provided significant insight into the excited-state properties of spheroidene and the photosynthetic reaction centers[34] including the homodimer special pair where the change in polarizability dominates the change in electric dipole moment upon electronic excitation.

Several theoretical approaches have been applied to the calculation of excited electronic state properties of polyene systems. Response theory has been employed to calculate the excited-state static and dynamic polarizabilities for a series of polyenes,[35] whereas for s-tetrazine, the electronic properties of the ground and first excited states were determined using the complete active space and the second-order multiconfiguration perturbation theory.[36] In the polyene study,[33] it was predicted that the first excited-state polarizability was nearly double that of the ground state and that the proximity to the manifold of higher excited states dominated this difference. For tetrazine,[34] the polarizability in the first excited state was a factor 1.12 greater than that of the ground state. This is due to the change in polarizability being confined to the molecular plane for the $n \rightarrow \pi^*$ transition. Our results are consistent with these predictions for conjugated π systems.

Anomalous Aqueous Spectra. The spectra of B(*a*)P in aqueous solution are of specific interest because of their curious behavior. In both the excitation and emission spectra, the intensity pattern is considerably different than that in any "pure" nonpolar or polar solvent. The effect is most pronounced in the emission spectrum, as shown in Figure 6 where the spectra in phosphate buffer and in hexane are compared. It is clear that the second member of the progression has become the most intense feature in buffer solution. Moreover, its shape and position have changed, shifting significantly to the red. This is in comparison with the other spectral features, which also red-shift with respect to those in hexane solution, but much less so.

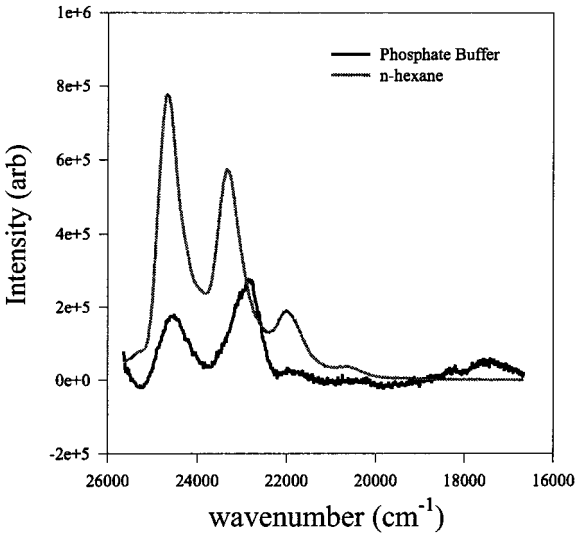

Figure 6. Fluorescence spectra of benzo[*a*]pyrene in 10^{-9} M phosphate buffer and in 10^{-6} M *n*-hexane. Note the shift and shape change in peak 2 for the buffer solution. In both cases B(*a*)P was excited at 380 nm.

It is also of value to compare the relative peak intensities for the two solutions. While the ratio of peaks 1 and 3 stays relatively constant (2.85 vs 2.36 for aqueous vs hexane), the ratios involving peak 2 are quite different (0.68 vs 1.21 for aqueous vs hexane). It is clear that peak 2 is a sensitive reporter of an aqueous environment. We will next consider possible explanations of this behavior.

Since the anomalous spectral features also occur in buffer solution, it is possible that the ions in the buffer solution have an effect on the spectra of B(*a*)P. Perhaps the bay region of B(*a*)P serves as a chelating site for an ionic species. The proximity of this ion could certainly affect the local vibrational potential energy surface for a stretching mode. We have attempted to determine the dependence of the spectrum on the concentration of EDTA and/or ions present in aqueous solution but found none. In fact, the spectra noted in Figure 6 are obtained when the aqueous solution is dilute enough that only isolated B(*a*)P is present; i.e., there would be very little aggregation. Therefore, there must be something specific about the interaction of water and B(*a*)P, as water is the only species present in all three solutions (neat H_2O, TE buffer, and phosphate buffer) that displays this behavior.

Upon close examination of the fluorescence spectra in phosphate buffer and hexane, it is notable that the shape of peak 2 has also changed. This could indicate that there is an enhancement of the Franck−Condon overlap for vibrational structure that was weak in other solvents. Such structure has been observed in the jet-cooled fluorescence spectrum of B(*a*)P but was not assigned. The fundamental energy of this mode is about 2200 cm^{-1}. From Gittins et al.,[19] there appears to be no fundamental vibration with this energy; therefore, it is likely a combination vibration. The enhancement of this transition could arise from a solvent-induced change in symmetry similar to that observed for solvation of pyrene.[37]

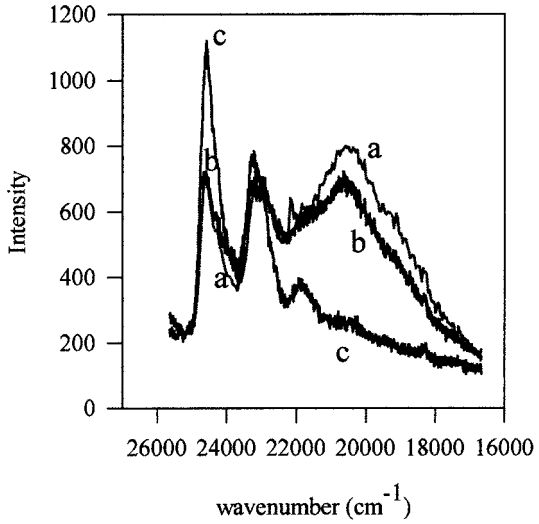

Figure 7. Emission spectra of 10^{-8} M B(*a*)P in TE buffer with various concentrations of dsDNA. Plots a−c represent 1×10^{-8}, 3×10^{-8}, and 5×10^{-7} M DNA, respectively. The excitation wavelength was 380 nm for all spectra.

B(*a*)P−DNA Interactions. The emission spectra of solutions of 10^{-8} M B(*a*)P over a series of 14 base pair dsDNA (3′-ATATAAATTTATAT-5′) concentrations in TE buffer are presented in Figure 7. Since the solubility of B(*a*)P is only 10^{-9} M, it is not surprising to see evidence of aggregates in the fluorescence spectrum. This appears as a red-shifted broad feature that peaks around 490 nm. The red-shifting is presumably due to excimer formation in the aggregate. The evidence for B(*a*)P association with DNA in TE buffer is the loss of intensity from the aggregate peak and increase in the intensities of the resolved peaks. The resolved spectral features present an intensity pattern that is similar to that of B(*a*)P in nonaqueous solution. Moreover, the fluorescence spectral features are broader than for any other solvent system. Equilibration of B(*a*)P uptake by DNA is a slow procession. Our solutions took several days to achieve steady state. This is largely because of the slow dissolution of B(*a*)P into aqueous solution. The situation is exacerbated if there is an activation barrier for association between single B(*a*)P and DNA molecules owing to its polyionic nature. Moreover, DNA could have a stronger interaction with the aggregates than monomers and solvate them in solution. At the B(*a*)P concentration used, it is unlikely that the aggregates are larger than trimers. Trimers would still be considerably smaller than the DNA oligomer. Therefore, it is valid to identify the association process with the binding of B(*a*)P to DNA, rather than the binding of DNA to larger microcrystals. In this scenario, some of the bound aggregates must be converted to monomeric B(*a*)P, as indicated by the increasing intensity of monomer spectrum with DNA concentration. Since the gain in monomer intensity is not exponentially proportional to the aggregate loss, some of the binding sites may be nonfluorescent. Nonfluorescent binding sites have reported the binding of ethidium to DNA.[38] If one is to estimate the association constant of B(*a*)P to dsDNA, one should therefore use the aggregate loss as an indication of bound B(*a*)P. In so doing, the association constant for B(*a*)P aggregates to DNA is determined to be approximately 1×10^7 M^{-1}. This number is not unreasonable compared with that of other aromatic molecules associating with poly(AT), DNA. For example, ethidium has a binding constant of 1.1×10^6 M^{-1}, including both fluorescent and nonfluorescent association.[38] The more severe hydrophobicity of B(*a*)P presumably drives its equilibrium even more in favor of association.

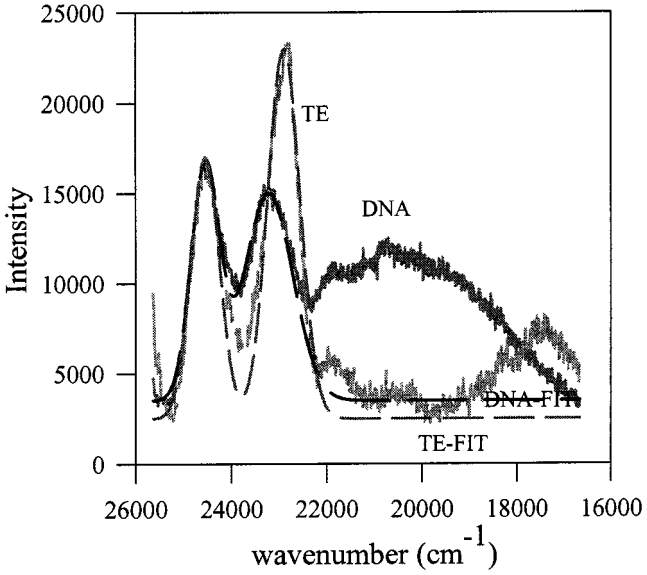

Figure 8. Fluorescence spectra of 10^{-8} M B(*a*)P in TE buffer and DNA/TE solutions (solid lines). Included are Gaussian-shaped lines fitted to the first two peaks of the spectra (dashed lines). The second peak is notably wider for the DNA solution. The excitation wavelength was 380 nm for both solutions. The spectra are normalized for ease of comparison.

It is interesting to speculate on the environment of the DNA-solvated B(*a*)P. Therefore, we have fitted Gaussian line shapes to the spectra to determine their positions and widths. The comparison is shown in Figure 8. The line-width at half-maximum for TE buffer is 800 cm^{-1}, whereas for DNA it is 1200 cm^{-1}. This may indicate the existence of multiple binding environments between DNA and B(*a*)P. We have observed[39] that in sodium dodecyl sulfate solutions, B(*a*)P avoids the negatively charged surfaces of the micelles and partitions almost exclusively into their lipophilic interiors. If B(*a*)P is associating with DNA, a reasonable hypothesis is that it will partition toward the base pairs and away from the negatively charged phosphate-sugar backbone. In fact, the peak positions and intensity ratios observed in these spectra resemble those seen in nonaqueous and micelle solutions.

The shifting of the spectrum of DNA "solvated" B(*a*)P suggests that the environment is similar to that of methanol and/or acetonitrile. The binding may be either intercalation, groove binding, or both. Since the peak is shifted 40 cm^{-1} from the TE buffer position, B(*a*)P is experiencing an environment different from that of the pure buffer. It is interesting to predict what the shift would be if B(*a*)P was bound to DNA in a classical intercalation site similar to that of ethidium. This would put 4 adenine and/or thymine bases spaced approximately 4 Å away from B(*a*)P, which is the molecular plane to molecular plane distance for classic intercalation. To compare this with our model, we need to examine the distance between the centers of polarizabilities. This will be the hypotenuse (7.6 Å) of the triangle whose other sides are 4 and 6.5 Å or half the long axis of B(*a*)P. Using the data of Pullman et al.[29] and our determined excited-state polarizability, we calculate a maximum shift of approximately 40 cm^{-1}. The actual measured value is 175 cm^{-1}. This incongruity could arise from the fact that our model would not account for the favorable, nonisotropic, π-stacking van der Waals interactions necessarily present with intercalation. Minor groove binding is another DNA-association motif found for small aromatic molecules such as Hoescht 33258.[40] This seems unlikely because B(*a*)P does not possess the curved structure inherent in every other known minor groove binding molecule.[40]

Moreover, the polar environment of the minor make it energetically less favorable for B(*a*)P than the intercalation sites.

4. Conclusions

In this paper, we have presented the solvatochromic shifts for benzo[*a*]pyrene in a series of polar and nonpolar solvents. The shifting of excitation and emission spectra are interpreted in terms of dispersive (London) interactions between B(*a*)P in its ground and excited electronic states and the solvent molecules in the first solvation shell. Thus, it was possible to estimate the excited-state static polarizability for B(*a*)P in the S_1, S_2, and S_3 states. We have observed an anomalous intensity pattern in both the emission and excitation spectra for B(*a*)P dissolved in aqueous solution and in aqueous buffer. This is attributed to solvent−solute interactions that alter the vibrational overlap between the ground and first excited electronic states. Finally, we have presented spectroscopic evidence of an interaction between B(*a*)P and double-stranded DNA in Tris/EDTA buffer.

Acknowledgment. This work is supported by the Natural Sciences and Engineering Research Council of Canada. Financial assistance from the University of Calgary is also gratefully appreciated. The authors would like to thank Professors S. Lees-Miller, D. Armstrong, and R. Paul (U. of Calgary) for stimulating discussions and Professor A. Okey (U. of Toronto) for the donation of benzo[*a*]pyrene. We also thank Professor Arvi Rauk (U. of Calgary) for his help in performing the dipole moment calculations. The authors are indebted to Professor G. Liu (U. of Calgary) for the use of his spectrometer.

References and Notes

(1) Okey, A. B.; Riddick, D. S.; Harper, P. A. *Trends Pharmacol. Sci*. **1994**, *15*, 226.
(2) Eriksson, M.; Eriksson, S.; Nordén, Jernström, B.; Gräslund, A. *Biopolymers* **1990**, *29*, 1249.
(3) Ridler, P. J.; Jennings, B. R. *Phys. Med. Biol.* **1983**, *28*, 625.
(4) Green, B.; McCarter, J. A. *J. Mol. Biol.* **1967**, *29*, 447.
(5) Nosaka, Y.; Kira, A.; Imamura, M. *J. Phys. Chem.* **1981**, *85*, 1353.
(6) Hyun, K. M.; Choi, S. D.; Lee, S.; Kim, S. K. *Biochim. Biophys. Acta* **1997**, *1334*, 312.
(7) Gallagher, S. H.; Armstrong, R. S.; Lay, P. A.; Reed, C. A. *J. Phys. Chem.* **1995**, *99*, 5817.
(8) Tetreault, N.; Muthyala, R. S.; Liu, R. S. H.; Steer, R. P. *J. Phys. Chem. A* **1999**, *103*, 2524.
(9) Stryer, L. S. *J. Mol. Biol.* **1965**, *13*, 482.
(10) McCrae, E. G. *J. Phys. Chem.* **1957**, *61*, 562.
(11) Capomacchia, A. C.; White, F. L.; Sobol, T. L. *Spectrochimica Acta* **1982**, *38a* (5), 513.
(12) Kamlet, M. J.; Abboud, J. L.; Taft, R. W. *J. Am. Chem. Soc.* **1977**, *99* (18), 6027.
(13) Bayliss, N. S.; McCrae, E. G. *J. Phys. Chem.* **1954**, *58*, 1002.
(14) Longuet-Higgins, H. C.; Pople, J. A. *J. Chem. Phys.* **1957**, *27* (1), 192.
(15) Lippert, E. *Z. Elektrochem.* **1957**, *61*, 962.
(16) Mataga, N.; Kaifu, Y.; Koizumi, M. *Bull Chem. Soc. Jpn.* **1956**, *29*, 465.
(17) Iball, J.; Scrimgeour, S. N.; Young, D. W. *Acta Crystallogr. B* **1976**, *32*, 325.
(18) Clar, E., *Polycyclic Hydrocarbons*; Academic Press: New York, 1964.
(19) Gittins, C.M.; Rohlfing, E. A.; Rohlfing, C. M. *J. Chem. Phys.* **1996**, *105*, 7323.
(20) Weber, G.; Laurence, D. J. R. *Biochem. J.* **1954**, *18*, 3075.
(21) Gaussian 98, Revision A.7; M. J. Frisch, G. W. Trucks, H. B. Schlegel, G. E. Scuseria, M. A. Robb, J. R. Cheeseman, V. G. Zakrzewski, J. A. Montgomery, Jr., R. E. Stratmann, J. C. Burant, S. Dapprich, J. M. Millam, A. D. Daniels, K. N. Kudin, M. C. Strain, O. Farkas, J. Tomasi, V. Barone, M. Cossi, R. Cammi, B. Mennucci, C. Pomelli, C. Adamo, S. Clifford, J. Ochterski, G. A. Petersson, P. Y. Ayala, Q. Cui, K. Morokuma, D. K. Malick, A. D. Rabuck, K. Raghavachari, J. B. Foresman, J. Cioslowski, J. V. Ortiz, A. G. Baboul, B. B. Stefanov, G. Liu, A. Liashenko, P. Piskorz, I. Komaromi, R. Gomperts, R. L. Martin, D. J. Fox, T. Keith, M. A. Al-Laham, C. Y. Peng, A. Nanayakkara, C. Gonzalez, M. Challacombe, P. M. W. Gill, B. Johnson, W. Chen, M. W. Wong, J. L. Andres, C. Gonzalez, M. Head-Gordon, E. S. Replogle, and J. A. Pople, Gaussian, Inc, Pittsburgh, PA, 1998.
(22) Eyring, H.; Walter, J.; Kimball, G. E. *Quantum Chemistry*; John Wiley and Sons: London, 1944.
(23) Kettley, J. C.; Palmer, T. F.; Simons, J. P.; Amos, T. A. *Chem. Phys. Lett*. **1986**, *126*, 107.
(24) Iweibo, I.; Chongwain, P. T.; Obi-Egbedi, N. O.; Lesi, A. F. *Spectrochim. Acta* **1991**, *47A*, 705.
(25) Abe, T. *Bull. Chem. Soc. Jpn.* **1965**, *38*, 1314.
(26) White, C. M.; Schmidt, C. E. *Fuel* **1987**, *66*, 1030.
(27) Imasaka, T.; Fukuoka, H.; Hatashi, T.; Ishibashi, N. *Anal. Chim. Acta* **1984**, *156*, 111.
(28) Greenblatt, G.D.; Nissani, E.; Zaroura, E.; Haas, Y. *J. Phys. Chem.* **1987**, *91*, 570.
(29) Pullman, B.; Claverie, P.; Caillet, J. *Science* **1965**, *107*, 1305.
(30) Andrews, J. R.; Hudson, B. S. *J. Chem. Phys.* **1978**, *68*, 4587.
(31) Norman, P.; Jonsson, D.; Ågren, H. *Chem. Phys. Lett.* **1997**, *268*, 337.
(32) Li, F..; Song,, Y.; Yang, K.; Liu, S.; Li, C. *Opt. Commun.* **1998**, *145*, 53.
(33) Bublitz, G.; Boxer, S. G. *Annu. Rev. Phys. Chem*. **1997**, *48*, 213.
(34) Lao, K.; Moore, L. J.; Zhou, H.; Boxer, S. G. *J. Phys. Chem*. **1995**, *99*, 496.
(35) Jonsson, D.; Norman, P.; Luo, Y.; Ågren, H. *J. Chem. Phys.* **1996**, *105*, 581.
(36) Schütz, M.; Hutter, J.; Lüthi, H. P. *J. Chem. Phys.* **1995**, *103*, 7048.
(37) Nakajima, A. *Bull. Chem. Soc. Jpn*. **1971**, *44*, 3272.
(38) Borisova, O. F.; Shchyolkina, A. K.; Karapetyan, A. T.; Surovaya, A. N. *Mol. Biol*. **1998**, *32*, 718.
(39) Cramb, D. T.; Beck, S. C. *J. Photochem. Photobiol. A* **2000**, in press.
(40) Vega, M. C.; Garcia Saez, I.; Aymami, J.; Eritja, R.; Van der Marel, G. A.; Van Boom, J. H.; Rich, A.; Coll, M. *Eur. J. Biochem*. **1994**, *222*, 721.
(41) Weast, R. C., Ed. *Handbook of Chemistry and Physics*; CRC Press: Boca Raton, FL, 1998.